Journal of the Serbian Society for Computational Mechanics / Special Edition / Vol. 10 / No. 1, 2016 / pp. 20-33

(UDC: 616.13-004.6-073
004.921)

A summary of results in modeling plaque formation and development, cochlea mechanics and vestibular disorders

N. Filipovic[1,2*], M. Radovic[1,2], V. Isailovic[1,2], Z. Milosevic[1,2], D. Nikolic[2], I. Saveljic[1,2], M. Nikolic[1], T. Djukic[2], B. Andjelkovic-Cirkovic[1], T. Exarchos[3], N. Meunier[4], Z. Teng[5], D. Fotiadis[3], F. Böhnke[6], O. Parodi[7]

[1] Faculty of Engineering, University of Kragujevac, Kragujevac, Serbia,
e-mail: fica@kg.ac.rs
[2] Bioengineering R&D Center, BioIRC, Serbia
[3] University of Ioannina, Ioannina, Greece
[4] University Paris Descartes, Paris, France
[5] University of Cambridge, Cambridge, Great Britain
[6] Department of Otorhinolaryngology, Technical University Munich, 22 Ismaningerstr, 81664 München, Germany
[7] National Research Council Pisa, Italy
**corresponding author*

Abstract

In this review we present scientific results from three EC FP7 projects: ARTREAT, SIFEM and EMBALANCE. The title of FP7 ARTREAT project was: Multi-level patient-specific artery and atherogenesis model for outcome prediction, decision support treatment, and virtual hand-on training. Researchers from the University of Kragujevac and BioIRC participated in this project. The original method for plaque formation and development was developed and validated on the pilot study patients for coronary and carotid arteries in EU clinical centers. Another FP7 project was SIFEM with the title: Semantic Infostructure interlinking an open source Finite Element tool and libraries with a model repository for the multi-scale Modelling and 3d visualization of the inner-ear. Methodology for cochlea model with tapered and rectangular basilar membrane with passive and active model was developed.

The main part of EMBALANCE FP7 project was modelling of vertigo diseases. Three-dimensional biomechanical model of semi-circular canals was described with full 3D fluid-structure interaction of particles, wall, cupula deformation and endolymph fluid flow. The model is compared with clinical data and nystagmus measurement on the vertigo patients.

Keywords: atherosclerosis, plaque formation, computer modeling, cochlea, passive and active model, vertigo disease, BPPV, nystagmus

1. Introduction

Atherosclerosis is a progressive disease described as the accumulation of lipids and fibrous elements in the large arteries. Although in the past the focus was on luminal narrowing because

of the bulk of atheroma, currently, the biological attributes of the atheroma are recognized as key determinants of its clinical significance (Libby 2002).

The process of inflammation begins with penetration of low density lipoproteins (LDL) in the intima. If it is too high, the penetration is followed by leucocyte recruitment in the intima. One endothelial-leukocyte adhesion molecule proved to be especially significant for the early adhesion of mononuclear leukocytes to arterial endothelium at places of atheroma initiation: Vascular cell adhesion molecule-1 (VCAM-1). The process itself might take part in the formation of the fatty streak, the initial lesion of atherosclerosis and, consequently, in the plaque formation (Kedem and Katchalsky 1961).

In ARTREAT project, we conducted computational study of plaque composition and initial progression. The aim of the project was to connect LDL transport with macrophages and oxidized LDL distribution and initial plaque grow model inside the intimal area. Mass transport of LDL through the wall and the simplified inflammatory process was solved first. The Navier-Stokes equations govern the blood motion in the lumen; the Darcy law was used for model blood filtration and Kedem-Katchalsky equations (Kedem and Katchalsky 1961; Kedem and Katchalsky 1958) for the solute and flux exchanges between the lumen and the intima. The system we used contained three additional reaction-diffusion equations that model the inflammatory process and lesion growth model in the intima. This model relies on a matter incompressibility assumption. Some examples of our simulation for plaque formation and progression are given in the results section (Filipovic et al. 2012; Filipovic et al. 2013).

In the SIFEM project we modeled cochlea mechanics. Cochlea is the most important part of the hearing system, since signal transduction into neural impulse occurs inside of it. Nerve impulses send information about input signal to the brain (von Békésy 1960). Human ear can distinguish input frequencies in range from 16 Hz to 20 kHz. The cochlea has shape like a snail and consists of three chambers filled with fluid – scala vestibuli, scala media and scala tympani, separated by two membranes – basilar membrane (BM) and Reissner's membrane. Inside of scala media the organ of Corti (OC) is placed, where generation of the electrical current and innervation of the auditory nerve occurs.

Cochlea is a much more complex organ than the external and middle ear. The basic structure is revealed in the cross-sectional sketch of a radial slice presented in Fig. 1. The cochlear partition that separates the cochlear fluid duct into three chambers, comprises the BM and the OC. The BM consists of a number of fibers oriented in radial directions. These transverse BM filers are inserted into the bony spiral lamina on the modulus end and the spiral ligament on the opposite side. The BM is narrower and thicker in the base than in the apex which imparts the stiffness gradient of the BM.

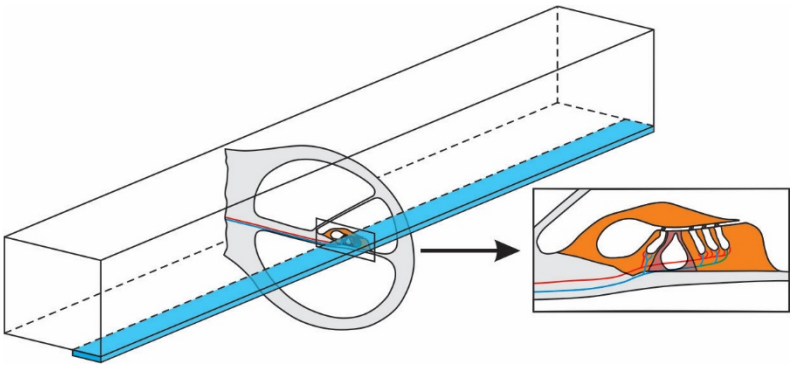

Fig 1. Anatomy of the cochlea for box model with the cross-sectional sketch of a radial slice

The cochlear models imitate the pressure wave moving along the BM with a focus on the vibrations of the cellular and membranous components of the cochlear partition (Diependaal and Viergever 1989; Geisler and Sang 1995; Yoon et al. 2007). The feed-forward micromechanics model takes into account the tilt of the outer hair cells (OHC) in the longitudinal direction along the cochlear duct and the resulting force in the BM.

Working on the EMBALANCE project, we modeled Benign Paroxysmal Positional Vertigo (BPPV). It is the most commonly diagnosed vertigo disease which means that basophilic particles exist in the semicircular canals (Berthoz 2002). Three-dimensional eye movement recordings and selective semicircular canal inactivation were utilized for investigation of the spatial organization of vestibular signals in the vestibulo-ocular reflex. BPPV develops most often in the posterior canal which is identified clinically by transient vertical-torsional nystagmus evoked with the Dix-Hallpike maneuver. The horizontal canal variant of BPPV is characterized by acute vestibular symptoms occuring during activities that reorient the HC relative to gravity, such as rolling over in bed (Baloh et al. 1993; Nuti et al. 1998; Pagnini et al. 1989).

After angular movements of the head the symptoms of BPPV typically appear. BPPV disease leads to dizziness, nausea and imbalance. It affects a considerable percentage of the whole population and especially elderly people. BPPV is diagnosed by tracking the eye movements during and after a head maneuver (nystagmus). The nystagmus actually aims to compensate any angular motion in order to stabilize our vision. Fluid mechanics and sedimenting particles tracking in a SCC are schematically presented in Fig. 1. It can be seen that sedimenting particles can move with the fluid motion and gravity through the SCC and they can hit the cupula and make unpleasant sensation which causes dizziness.

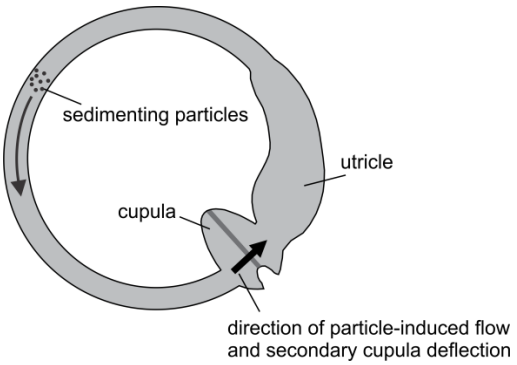

Fig. 2. Fluid mechanics and sedimenting particles tracking in a semicircular canal

2. Materials and methods

2.1 Modeling of plaque formation and progression

In this section, we present mass transfer problem for LDL transport through the wall first and then a continuum based approach for plaque formation and development in three-dimension is described. The governing equations and numerical procedures are given. The blood flow in lumen domain is simulated by the three-dimensional Navier-Stokes equations, together with the continuity equation:

$$-\mu\nabla^2 u_l + \rho(u_l \cdot \nabla)u_l + \nabla p_l = 0 \tag{1}$$

$$\nabla u_l = 0 \tag{2}$$

where $\boldsymbol{u}_l$ is blood velocity in the lumen, p_l is the pressure, μ is the dynamic viscosity of the blood, and ρ is the density of the blood.

Mass transfer in the blood lumen is coupled with the blood flow and modeled by the convection-diffusion equation as follows:

$$\nabla \cdot \left(- D_l \nabla c_l + c_l u_l \right) = 0 \tag{3}$$

in the fluid domain, where c_l is the solute concentration in the blood domain, and D_l is the solute diffusivity in the lumen.

Mass transfer in the arterial wall is coupled with the transmural flow and modeled by the convection-diffusion-reaction equation as follows:

$$\nabla \cdot \left(-D_w \nabla c_w + k c_w u_w \right) = r_w c_w \tag{4}$$

in the wall domain, where c_w is the solute concentration in the arterial wall, D_w is the solute diffusivity in the arterial wall, k is the solute lag coefficient, and r_w is the consumption rate constant.

LDL transport in lumen of the vessel is coupled with Kedem-Katchalsky equations (Kedem and Katchalsky 1961; Kedem and Katchalsky 1958):

$$J_v = L_p \left(\Delta p - \sigma_d \Delta \pi \right) \tag{5}$$

$$J_s = P \Delta c + \left(1 - \sigma_f \right) J_v \bar{c} \tag{6}$$

where J_v is the transmural velocity, J_s is the solute flux, L_p is the hydraulic conductivity of the endothelium, Δc is the solute concentration difference across the endothelium, Δp is the pressure drop across the endothelium, $\Delta \pi$ is the oncotic pressure difference across the endothelium, σ_d is the osmotic reflection coefficient, σ_f is the solvent reflection coefficient, P is the solute endothelial permeability, and $\bar{c}$ is the mean endothelial concentration.

In our simulations we used a single layer model while multilayered model is still under development. The first term in Kedem-Katchalsky equations $P \Delta c$ of the right hand side in (Eq. 6) defines the diffusive flux across the endothelium, while the second term $\left(1 - \sigma_f \right) J_v \bar{c}$ defines the convective flux. Here, we did not neglect the convective term. Only the oncotic pressure difference $\Delta \pi$ was neglected because of decoupling the fluid dynamics from solute dynamics. We used the incremental-iterative procedure to treat the convective diffusion terms for LDL transport.

The inflammatory process was solved using three additional reaction-diffusion partial differential equations (Filipovic et al. 2012; Filipovic et al 2013):

$$\begin{aligned} &\partial_t Ox = d_1 \Delta Ox - k_1 Ox \cdot M \\ &\partial_t M + div(v_w M) = d_2 \Delta M - k_1 Ox \cdot M + S / (1 + S) \\ &\partial_t S = d_3 \Delta S - \lambda S + k_1 Ox \cdot M + \gamma (Ox - Ox^{thr}) \end{aligned} \tag{7}$$

where Ox is the oxidized LDL or c_w - the solute concentration in the wall from Eq. (4); M and S are concentrations in the intima of macrophages and cytokines, respectively; d_1, d_2, d_3 are the corresponding diffusion coefficients; λ and γ are degradation and LDL oxidized detection coefficients; and v_w is the inflammatory velocity of plaque growth, which satisfies Darcy's law and continuity equation (Filipovic et al. 2012; Filipovic et al 2013):

$$v_w - \nabla \cdot (p_w) = 0 \tag{8}$$

$$\nabla v_w = 0 \tag{9}$$

in the wall domain. Here, p_w is the pressure in the arterial wall.

2.2 Mathematical model of the cochlea

To describe mechanical behavior of the cochlea, acoustic equation (Elliott et al. 2013) for describing fluid inside the chambers was used together with Newtonian dynamics equation for describing vibration of the BM, a solid part of the model. The acoustic wave equation is given below:

$$\frac{\partial^2 p}{\partial x_i^2} - \frac{1}{c^2}\frac{\partial^2 p}{\partial t^2} = 0 \tag{10}$$

where p is fluid pressure, c stands for speed of sound, x_i are spatial coordinates in all three Cartesian directions ($i = 1,2,3$) and t is time. Equation (10) can be presented in the matrix form:

$$\mathbf{Q}\ddot{\mathbf{p}} + \mathbf{H}\mathbf{p} = \mathbf{0} \tag{11}$$

In equation (11) $\mathbf{Q}$ and $\mathbf{H}$ are acoustic inertia matrix and acoustic stiffness matrix, respectively.

Solid motion was described using Newtonian dynamics equation:

$$\mathbf{M}\ddot{\mathbf{U}} + \mathbf{B}\dot{\mathbf{U}} + \mathbf{K}\mathbf{U} = \mathbf{F}^{ext} \tag{12}$$

$\mathbf{M}$, $\mathbf{B}$ and $\mathbf{K}$ are mass, damping and stiffness matrices, $\mathbf{U}$ is displacement vector, $\dot{\mathbf{U}}$ is velocity vector, $\ddot{\mathbf{U}}$ is acceleration vector and $\mathbf{F}^{ext}$ is vector of external forces, applied at the BM.

The applied type of the analysis was modal analysis, where damping matrix could be included inside the stiffness matrix as a complex, imaginary part. In that way, Eq. (12) can be written in the following form:

$$\mathbf{M}\ddot{\mathbf{U}} + \mathbf{K}(1 + i\eta)\mathbf{U} = \mathbf{F}^{ext} \tag{13}$$

In Eq. (13), η stands for hysteretic damping ratio, depending on the distance from the base of the BM.

The model was solved with the finite element method in PAK solver. Fluid and solid domain were strong coupled. The condition of coupling [17] was equalization of normal acceleration of the solid element to the normal pressure gradient of the fluid element, as it is written in equation (14):

$$\mathbf{n} \cdot \nabla p = \rho \mathbf{n} \cdot \ddot{u} \tag{14}$$

Finally, the coupled system of the equations has the form:

$$\begin{bmatrix} \mathbf{M} & 0 \\ -\rho_f \mathbf{R} & \mathbf{Q} \end{bmatrix} \begin{Bmatrix} \ddot{\mathbf{U}} \\ \ddot{\mathbf{p}} \end{Bmatrix} + \begin{bmatrix} \mathbf{K}(1+i\eta) & -\mathbf{S} \\ 0 & \mathbf{H} \end{bmatrix} \begin{Bmatrix} \mathbf{U} \\ \mathbf{p} \end{Bmatrix} = \begin{bmatrix} \mathbf{F} \\ \mathbf{q} \end{bmatrix} \tag{15}$$

In order to solve these second order equations we assumed sinusoidal solution for the displacement of the BM and for the pressure of the fluid:

$$\begin{aligned} \mathbf{U} &= \mathbf{A_U} \sin(\omega t + \alpha) \\ \mathbf{p} &= \mathbf{A_p} \sin(\omega t + \alpha) \end{aligned} \tag{16}$$

Substituing the assumed solution in equation (15), the system of linear equations [18] is obtained and solved in PAK solver.

$$\begin{bmatrix} \mathbf{K}(1+i\eta) - \omega^2 \mathbf{M} & -\mathbf{S} \\ -\rho_f \mathbf{R} & \mathbf{H} - \omega^2 \mathbf{Q} \end{bmatrix} \begin{Bmatrix} \mathbf{A_U} \\ \mathbf{A_p} \end{Bmatrix} = \begin{bmatrix} \mathbf{0} \\ \mathbf{q} \end{bmatrix} \tag{17}$$

2.3 Numerical procedure for fluid domain in SCC

For fluid domain inside SCC, the full 3D Navier-Stokes equation and continuity equation were used. To eliminate the number of unknowns and direct pressure calculation in the velocity-pressure formulation, the Penalty method was implemented (Kojic et al. 2008; Filipovic et al. 2006). The procedure is as follows. The continuity equation is approximated as:

$$v_{i,i} + \frac{p}{\lambda} = 0 \tag{18}$$

where λ is a selected large number, the penalty parameter. Substituting the pressure p from Eq. (18) into the Navier-Stokes equations, the following can be obtained:

$$\rho\left(\frac{\partial v_i}{\partial t} + \partial v_{i,k} v_k \right) - \lambda v_{j,ij} - \mu v_{i,kk} - f_i^V = 0 \tag{19}$$

then, the FE equation of balance becomes:

$$\mathbf{M}\dot{\mathbf{V}} + \left(\mathbf{K}_{vv} + \mathbf{K}_{vv}^{\lambda} \right) \mathbf{V} = \mathbf{F}_v + \mathbf{F}_{\lambda} \tag{20}$$

where

$$\left[K_{KJ}^{\lambda} \right]_{ik} = \lambda \int_V N_{K,i} N_{J,k} dV \quad , \left(\mathbf{F}_{\lambda} \right)_{Ki} = \lambda \int_S N_K v_{j,j} n_i dS \tag{21}$$

3. Results

3.1 Results for ARTREAT project

In the clinical study during ARTREAT project (**www.artreat.org**, **www.artreat.kg.ac.rs**) we examined plaque position for the coronary artery for baseline and follow-up time. The procedure also included stent position. Measurements were done with CT and the results were compared with computer simulation.

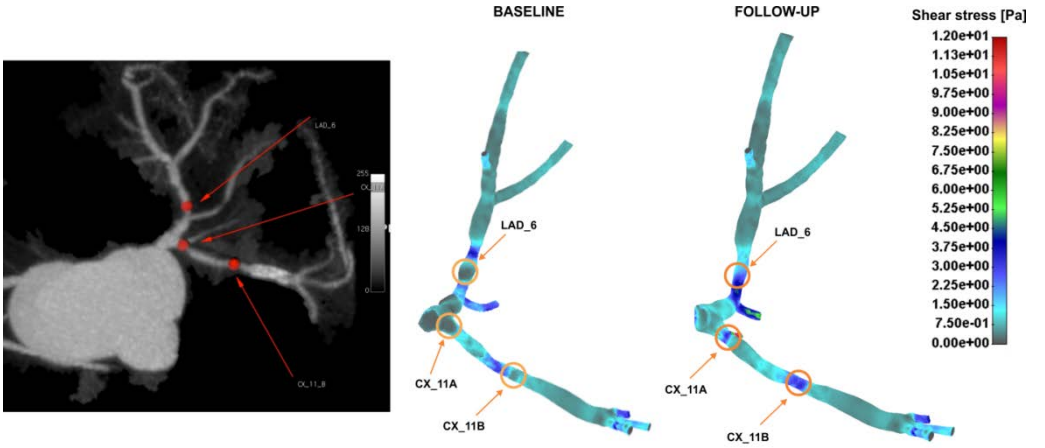

Fig. 3. Baseline and follow-up for plaque position at CX and LAD

Plaque position at CX and LAD artery for baseline and follow-up is presented in Fig. 3. Stent position can also be seen from the Fig. 4. Shear stress and plaque concentration for this patient is shown in Fig. 4. It can be seen that the plaque concentration on the specific cross-section location is matched with CT measurement.

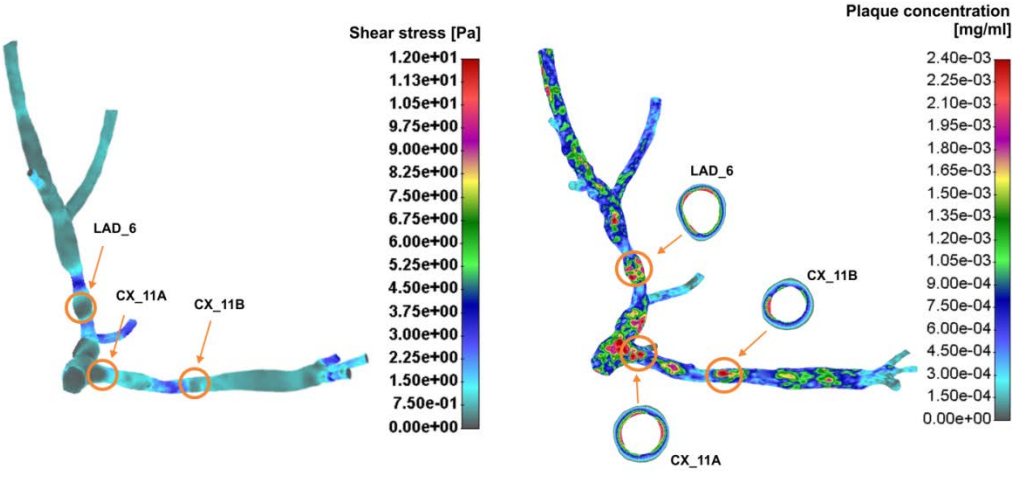

Fig. 4. Shear stress and plaque concentration for coronary artery patient

3.2 Results for SIFEM project

The tapered cochlea model was tested initially with air conduction excitation, via the outer ear. The obtained results are presented in Fig. 5.

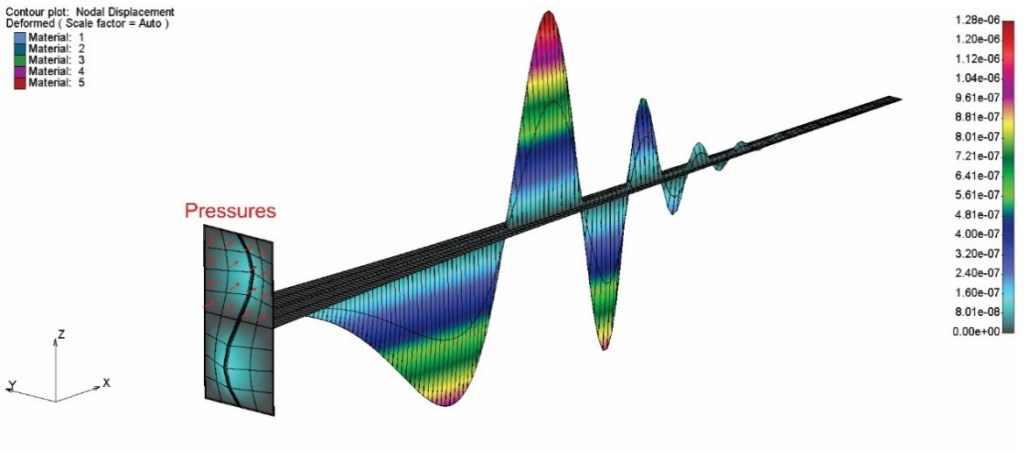

Fig. 5. Displacement wave of the basilar tapered membrane for applied input frequency of 1 kHz, air conduction simulation

In the bone conduction case, excitation originates from vibrations of the temporal bones, surrounding the cochlea. The results obtained for displacement vector applied in all three directions with unit magnitude and input frequency of 1 kHz are given in Fig. 6.

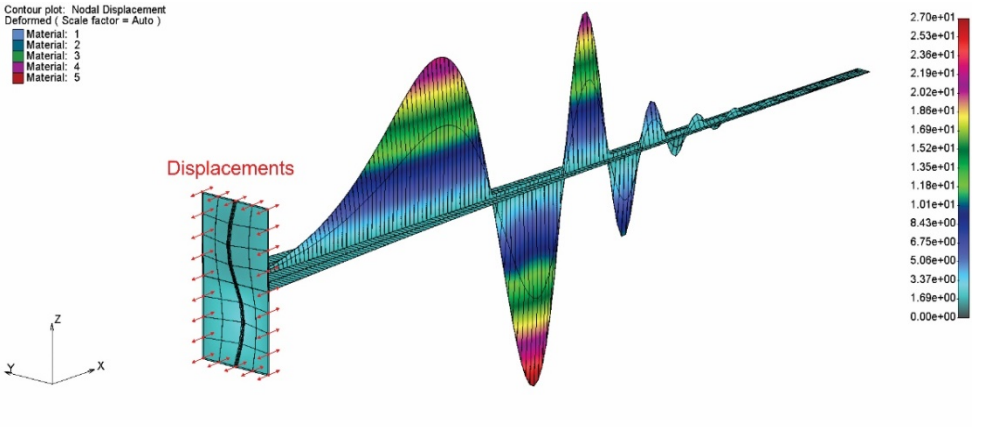

Fig. 6. Displacement wave of the basilar tapered membrane for applied input unit magnitude in all three directions and frequency of 1 kHz, bone conduction simulation

3.3 Results for EMBALANCE project

Patient geometry for all three SCC was reconstructed from DICOM images. Velocity distribution with several particles inside SCC is presented in Fig. 7. A different head motion can be used to get the response for all three SCC as shear stress distribution, velocity, cupula deformation and drag force on the wall.

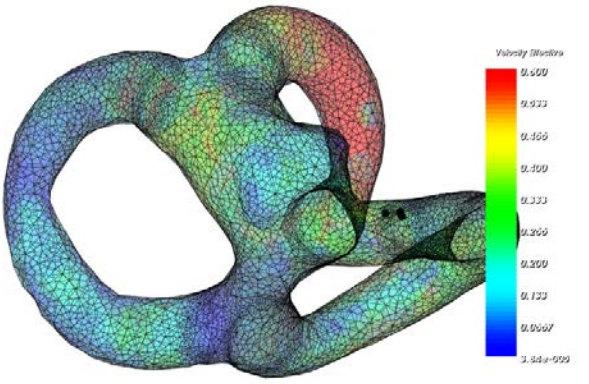

Fig. 7. Velocity distribution for BPPV patient

We tried to model diagnostic test which consists of four head rotations presented in Fig. 8. Five instants in time (I-V) for the diagnostic maneuver for BPPV where the patient was in the supine position were simulated with our model. After a short pause, the head was rotated in yaw 90° toward the affected ear, and then 180° yaw in the opposite direction. We modeled these movements by defining the series of consecutive discrete time steps with corresponding number of otoconia particles.

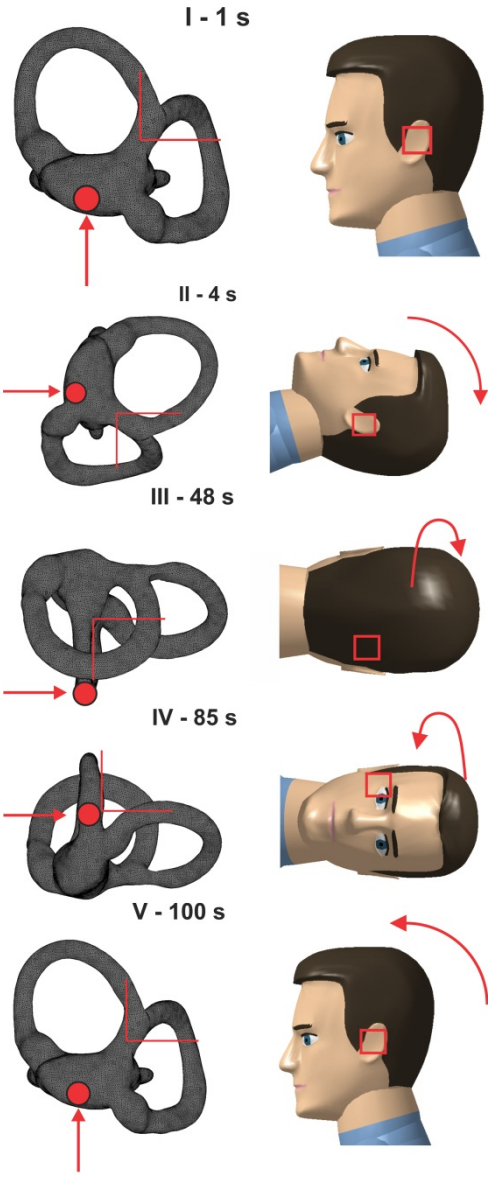

Fig. 8. The orientations of the membranous labyrinth at five instants in time (I-V) for the diagnostic maneuver

The corresponding head motion with canalith repositioning procedures moves the endolymph in all SCC. The flow induces the cupula deformation due to fluid forces which act on the cupula wall. Cupula volume displacement for the BPPV patient is shown in Fig. 9.

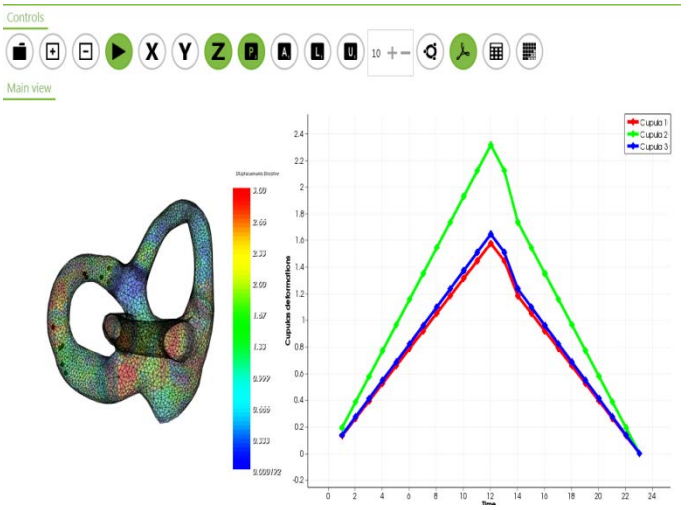

Fig. 9. Simulation of the otoconia particles motion and cupula deformation

4. Discussion and conclusion

In ARTREAT project, a full three-dimensional model for plaque formation and initial progression, coupled with blood flow and LDL concentration in blood, was developed. The Navier-Stokes equations and Darcy law for model blood filtration as well as Kedem-Katchalsky equations for the solute and flux transfer were implemented. Additionally, the system of three additional reaction-diffusion equations for simulation of the inflammatory process was coupled with full incremental iterative procedure. The wall permeability was assumed to be the function of wall shear stress with more permeability with low and oscillatory shear stress.

Patient specific study showed three different position of plaque location where low shear stress appear. Futhermore, after follow up, the size of simulated and measured plaque were matching. Computer analysis gave more insight for possible structure of the plaque. This study is a novel way of modeling plaque formation and development (Parodi et al. 2012). Matching the plaque location and progression in time between experimental and computer model shows a potential benefit for future prediction of this vascular decease using computer simulation.

In SIFEM project we developed a 3D FE model of the cochlea box model with tapered and rectangular BM. Models for both air and bone conduction were used to simulate mechanical behavior of the cochlea. The simplified active model with feed-forward and feedbackward OHC forces of tapered and rectangular box model was implemented. The passive model showed good matching with Greenwood function, which means that it can replicate frequency to place characteristic of the cochlea. The active model results presented BM velocity with respect to input stapes velocity for passive cochlea and it was in good agreement with measurement by Gundersen et al. (1978) and Stenfelt et al (2003).

In EMBALANCE project physiologically realistic description of the SCC, fluid motion, otoconia interaction with wall, fluid and cupula as well as cupula elastic deformation was described. There was no limit in size and number of otoconia particles which can be simulated. Fluid vortices were simulated inside the untricle and ampula which is almost impossible in the current dynamics models from the literature. Cupula deformation can be very complex deformation in 3D, not just integral from the flow domain as it was used in the previous studies (Rabbitt et al. 1994; Rabbitt 1999; Rabbitt et al. 2004). Simulation of many dynamics position of head with this model can give very precise position of fluid. Also, simulation of cupula

deflection directly corresponds to the nystagmus. This can help in better diagnostic process of BPPV disease.

Acknowledgments This review was funded by grants from EC: FP7-ICT-2007 224297 ARTREAT, FP7 ICT SIFEM 600933 and FP7 610454 EMBALANCE and grants from Serbian Ministry of Education, Science and Technological Development III41007 and ON174028.

Извод

Преглед резултата у области моделирања настанка и развоја плака, механике кохлее и поремећаја вестибуларног система

Н. Филиповић[1,2*], М. Радовић[1,2], В. Исаиловић[1,2], Ж. Милошевић[1,2], Д. Николић[2], И.Савељић[1,2], М. Николић[1], Т. Ђукић[2], Б. Анђелковић Ћирковић[1], T. Exarchos[3], N. Meunier[4], Z. Teng[5], D. Fotiadis[3], F. Böhnke[6], O. Parodi[7]

[1] Факултет инжењерских наука, Универзитет у Крагујевцу, Крагујевац, Србија
имејл: fica@kg.ac.rs
[2] Истраживачко-развојни центар за биоинжењеринг БиоИРЦ, Крагујевац, Србија
[3] University of Ioannina, Јањина, Грчка
[4] University Paris Descartes, Париз, Француска
[5] University of Cambridge, Кембриц, Велика Британија
[6] Department of Otorhinolaryngology, Technical University Munich, Минхен, Немачка
[7] National Research Council Pisa, Пиза, Италија
**главни аутор*

Резиме

У овом прегледном раду представљени су научни резултати три ФП7 пројекта Европске комисије: ARTREAT, SIFEM и EMBALANCE. Назив ФП7 ARTREAT пројекта био је: Моделирање и предвиђање артеросклерозе на вишеслојном моделу пацијента и виртуелно тренирање на фантому. Истраживачи са Универзитета у Крагујевцу и БиоИРЦ-а узели су учешће у овом пројекту. Оригинална метода за формирање и развој плака развијена је и потврђена пилот студијом у ЕУ клиничким центрима за лечење коронарних и каротидних артерија. Други ФП7 пројекат био је SIFEM са темом: Семантичко повезивање алата и библиотека методе коначних елемената отвореног кода са репозиторијумом за вишеслојни модел и 3Д визуализацију унутрашњег уха.

Развијена је методологија за модел кохлее са суженом и правом базиларном мембраном са пасивним и активним моделом. Главни део EMBALANCE ФП7 пројекта је био модел поремећаја код вертига. Тродимензиони модел полукружних канала је описан са 3Д интеракцијом солид-флуид са честицама, зидом, деформацијом купуле и ендолимфног флуида. Модел је поређен са клиничким подацима и мерењима нистагмуса на пацијентима који имају вертиго.

Кључне речи: артеросклероза, образовање плака, компјутерско моделирање, кохлеа, пасиван и активан модел, вертиго, БППВ (бенигни пароксизмални позициони вертиго), нистагмус

References

Baloh RW, Jacobson K, Honrubia V (1993). Horizontal semicircular canal variant of benign positional vertigo, *Neurology* 43, pp. 2542–2549.

Berthoz A (2002). *The sense of movement*. Harvard University Press.

Diependaal RJ, Viergever MA (1989). Nonlinear and active two-dimensional cochlear models: time-domain solution, *J Acoust Soc Am*, 85, 803–812.

Elliott SJ, Ni G, Mace BR, Lineton B (2013). A wave finite element analysis of the passive cochlea, *The Journal of the Acoustical Society of America*, 133(3), 1535-45.

Filipovic N, Mijailovic S, Tsuda A, Kojic M (2006). An implicit algorithm within the Arbitrary Lagrangian-Eulerian formulation for solving incompressible fluid flow with large boundary motions. *Comp. Meth. Appl. Mech. Eng*. 195:6347-6361.

Filipovic N, Rosic M, Tanaskovic I, Milosevic Z, Nikolic D, Zdravkovic N, Peulic A, Fotiadis D, Parodi O (2012). ARTreat project: Three-dimensional Numerical Simulation of Plaque Formation and Development in the Arteries, *IEEE Trans Inf Technol Biomed* 16(2):272-278.

Filipovic N, Teng Z, Radovic M, Saveljic I, Fotiadis D and Parodi O (2013). Computer simulation of three dimensional plaque formation and progression in the carotid artery, *Medical & Biological Engineering & Computing* DOI: 10.1007/s11517-012-1031-4.

Geisler CD, Sang C (1995). A cochlear model using feed-forward outer-hair-cell forces, *Hear Res*, 86, 132–146.

Gundersen T, Skarstein O, Sikkeland T (1978). A study of the vibration of the basilar membrane in human temporal bone preparations by the use of the Mössbauer effect, *Acta Otolaryngol*, 86(3–4), 225–232

Kaazempur-Mofrad MR, Ethier CR (2001). Mass transport in an anatomically realistic human right coronary artery, *Ann Biomed Eng* 29:121–127.

Kedem O, Katchalsky A (1958). Thermodynamic analysis of the permeability of biological membranes to non-electrolytes. *Biochim. Biophys* 27:229–246.

Kedem O, Katchalsky A (1961). A physical interpretation of the phenomenological coefficients of membrane permeability. *The Journal of General Physiology* 45:143–179.

Kojic M, Filipovic N, Stojanovic B, Kojic N (2008). *Computer Modeling in Bioengineering: Theoretical Background, Examples and Software*. John Wiley and Sons, Chichester, England.

Libby P (2002). Inflammation in atherosclerosis, *Nature*, 868–874.

Ni G (2012). Fluid coupling and waves in the cochlea, PhD thesis, University of Southampton, Faculty of engineering and the environment, Institute of sound and vibration research.

Nuti D, Agus G, Barbieri MT, Passali D (1998). The management of horizontal-canal paroxysmal positional vertigo, *Acta Otolaryngol* 118, pp. 455–460.

Pagnini P, Nuti D, Vannucchi P (1989). Benign paroxysmal vertigo of the horizontal canal, ORL J *Otorhinolaryngol Relat Spec*, 51, pp. 161–170.

PAK – Program for finite element analysis of cochlea mechanics (2015). BIOIRC doo Kragujevac, Serbia, SIFEM project, http://www.bioirc.ac.rs/index.php/sifem

Parodi O, Exarchos T, Marraccini P, Vozzi F, Milosevic Z, Nikolic D, Sakellarios A, Siogkas P, Fotiadis DI, Filipovic N (2012). Patient-specific prediction of coronary plaque growth from CTA angiography: a multiscale model for plaque formation and progression. *IEEE Transaction on Information Technology in Biomedicine* 16(5):952-965

Rabbitt RD (1999). Directional coding of three-dimensional movements by the vestibular semicircular canals, *Biol. Cybern*., 80(6), pp. 417–431.

Rabbitt RD et al. (2004). Hair-cell versus afferent adaptation in the semicircular canals. *J. Neurophysiol*., 93(1), pp. 424–436.

Rabbitt RD, Boyle R, Highstein SM (1994). Sensory transduction of head velocity and acceleration in the toadfish horizontal semicircular canal. *J. Neurophysiol*., 72(2), pp. 1041–1048.

Rabbitt RD, Damiano ER, Grant JW (2003). *Biomechanics of the vestibular semicircular canals and otolith organs*. In Highstein, S. M. A. Popper, & R. Fay (eds. The Vestibular System. Springer-Verlag New York, pp. 153–201.

Stenfelt S, Puria S, Hato N, Goode RL (2003). Basilar membrane and osseous spiral lamina motion in human cadavers with air and bone conduction stimuli, *Hear Res*, 181,131–143.

von Békésy G (1960). *Experiments in hearing*, New York: McGraw-Hill; 745.

Yoon, Y.J., Puria, S., Steele, C.R. (2007). Intracochlear pressure and derived quantities from a three-dimensional model, *J Acoust Soc Am*, 122(2), 952–966.

Zienkievich OC (1983). *The finite element method*, third edition, Published by McGraw-Hill Book Co., New York, ISBN 10:0070840725 / ISBN 13:9780070840720